Numerical Studies of Transport Properties through Artificial Atoms under Magnetic Fields

Mikio Eto

Department of Physics, Faculty of Science and Technology, Keio University
3-14-1 Hiyoshi, Kohoku-ku, Yokohama 223-8522, Japan
Phone: +81-45-563-1141 ex. 3981, Fax: +81-45-563-1761,
E-mail: eto@rk.phys.keio.ac.jp

1. Introduction

Recent microfabrication techniques have enabled us to make small quantum dots and control the number of electrons confined in a quantum dot. In a sufficiently small dot fabricated on a semiconductor, the energy level spacings are comparable with the charging energy. An atomic-like "shell structure" of the energy level distribution has been observed experimentally, using Coulomb oscillation, which is a peak structure of the conductance that occurs as a function of the gate voltage $V_{\rm gate}$ attached to the dot [1]. Hence small quantum dots are called artificial atoms. The fundamental research of the artificial atoms should be necessary for the application of small quantum dots to single-electron devices.

The purpose of the present paper is to elucidate the transport properties of the artificial atoms theoretically, to explain the experimental results by Tarucha *et al.* [1] and Kouwenhoven *et al.* [2]. To determine the electronic states in a small quantum dot, discrete energy levels and electron-electron Coulomb interaction have to be taken into account simultaneously. We adopt the exact diagonalization method to calculate not only ground state but also excited states as functions of magnetic field. The conductance is calculated using the obtained many-body states. With an increase in magnetic field, the electronic correlation becomes more important. The correlation effect on the transport properties is discussed.

2. Calculation Method

We consider N electrons which are confined in a two-dimensional harmonic potential and interact with each other. The magnetic field (H) is applied perpendicularly to the potential plane. The Hamiltonian reads

$$\mathcal{H} = \mathcal{H}_1 + \mathcal{H}_2, \tag{1}$$

$$\mathcal{H}_1 = \sum_i^N \left[\frac{1}{2m^*} \left(\mathbf{p}_i + \frac{e}{c}\mathbf{A}(\mathbf{r}_i) \right)^2 + \frac{1}{2} m^* \omega_0^2 \mathbf{r}_i^2 \right], \tag{2}$$

$$\mathcal{H}_2 = \sum_{i<j} \frac{e^2}{\varepsilon |\mathbf{r}_i - \mathbf{r}_j|}, \tag{3}$$

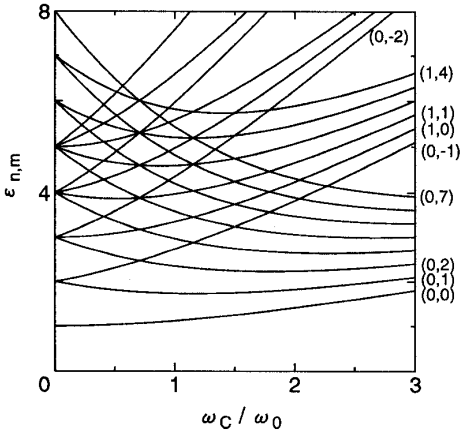

Figure 1: The magnetic field dependence of the one-electron levels, $\varepsilon_{n,m}$, in units of $\hbar\omega_0$. In the abscissa, $\omega_c = eH/m^*c$ is the cyclotron frequency. The radial and angular momentum quantum numbers, (n, m), are indicated.

where m^* is the effective mass of electrons and $\mathbf{A}(\mathbf{r})$ is the vector potential. The Zeeman effect is neglected.

The one-electron part of the Hamiltonian, $\mathcal{H}_1$, is first diagonalized to obtain one-electron energy levels. In the absence of magnetic field, the energy levels form shells, the nth shell of which consists of n degenerate levels, or $2n$ states if the electronic spins are counted. The level spacing is $\hbar\omega_0$, which is $\approx$ 5meV in the experiments [1,2]. The strength of the Coulomb interaction, $e^2/\varepsilon l_0$ where $l_0 = \sqrt{\hbar/m^*\omega_0}$ is the dot size, is comparable to the level spacing.

Under magnetic fields, the one-electron levels are expressed as

$$\varepsilon_{n,m} = \hbar\Omega(H)(2n + |m| + 1) - \frac{1}{2}\hbar\omega_c m, \tag{4}$$

0-7803-4369-7/98 $10.00

with

$$\Omega(H) = \sqrt{\omega_0^2 + \omega_c^2/4}, \tag{5}$$

where n and m are radial and angular momentum quantum numbers, respectively. $\omega_c = eH/m^*c$ is the cyclotron frequency. The magnetic field dependence of the levels is shown in Fig. 1. The magnetic field shrinks the wavefunctions as the magnetic length $l(H) = \sqrt{\hbar/m^*\Omega(H)}$.

The electron-electron interaction is taken into account by the exact diagonalization method [3-10]. The Hamiltonian, $\mathcal{H}$, is diagonalized in a restricted configuration space [11]. We obtain not only the ground state, $\Psi_{N,1}$ with energy $E_{N,1}$, but also low-lying excited states, $\Psi_{N,i}$, $E_{N,i}$ $(i = 2, 3, \cdots)$. The addition energies which are needed to place the Nth electron on the dot are given by

$$\mu_{N,i} = E_{N,i} - E_{N-1,1}. \tag{6}$$

$\mu_{N,1}$ corresponds to $E_{\rm gate} = -(-e)V_{\rm gate}$ at the Nth peak of the linear-conductance at $T = 0$. $\mu_{N,i}$ $(i \geq 2)$ can also be investigated experimentally by looking at differential conductance under finite bias voltages [2].

The conductance through a quantum dot is calculated, using the obtained many-body states, to the lowest order of the tunneling Hamiltonian which connects the dot and two external leads

$$\mathcal{H}_{\rm T}^{\rm L/R} = \sum_{k,l,\sigma} \left(T_l^{\rm L/R} c_{{\rm L/R},k,\sigma}^\dagger c_{l,\sigma} + {\rm h.c.} \right). \tag{7}$$

Here $c_{{\rm L/R},k,\sigma}^\dagger$ and $c_{{\rm L/R},k,\sigma}$ ($c_{l,\sigma}^\dagger$ and $c_{l,\sigma}$) are the creation and annihilation operators of state k in left/right lead (state $l = (n, m)$ in the dot) with spin σ. The linear-conductance is expressed as

$$G = \frac{e^2}{k_{\rm B}T} \sum_N \sum_{i,j} \frac{\Gamma_{N+1,j;N,i}^{\rm L} \Gamma_{N+1,j;N,i}^{\rm R}}{\Gamma_{N+1,j;N,i}^{\rm L} + \Gamma_{N+1,j;N,i}^{\rm R}} P_{N,i} \times f(E_{N+1,j} - E_{N,i} - E_{\rm gate} - E_{\rm F}), \tag{8}$$

where $P_{N,i}$ is the grand-canonical distribution function, $\exp[-(E_{N,i} - NE_{\rm gate})/k_{\rm B}T]/\Xi$, and f is the Fermi distribution function. The transition probability between states $\Psi_{N,i}$ and $\Psi_{N+1,j}$, with an electron tunneling through left/right barrier, is given by

$$\Gamma_{N+1,j;N,i}^{\rm L/R} = \frac{2\pi}{\hbar} D^{\rm L/R} \left| T_l^{\rm L/R} \right|^2 \left| \sum_{l,\sigma} \langle \Psi_{N+1,j} | c_{l,\sigma}^\dagger | \Psi_{N,i} \rangle \right|^2,$$

where $D^{\rm L/R}$ is the density of states in the left/right lead [12].

3. Calculated Results

Peak positions of the Coulomb oscillation

Figure 2 (a) shows peak positions of the Coulomb oscillation (addition energies, $\mu_{N,1}$), as functions of magnetic field. When the magnetic field is not too high,

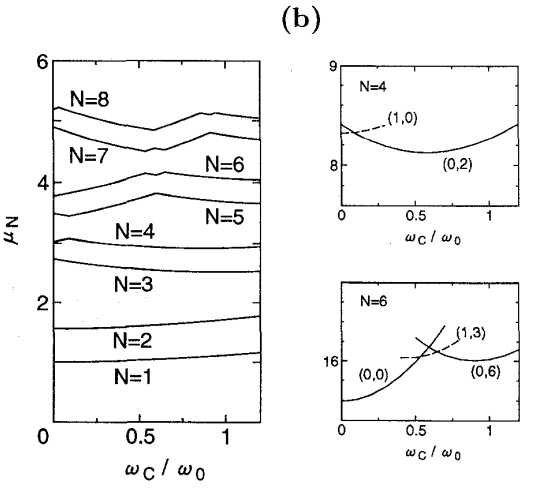

Figure 2: (a) Magnetic field dependence of the addition energies $\mu_{N,1}$ on a quantum dot. The unit of $\mu_{N,1}$ is $\hbar\omega_0$. In the abscissa, $\omega_c = eH/m^*c$ is the cyclotron frequency. (b) The ground state energies for $N = 4$ and $N = 6$ as functions of magnetic field. The total spin and total angular momentum, (S, M), are indicated for each state. [The strength of Coulomb interaction is $e^2/\varepsilon l_0 = \hbar\omega_0/2$.]

the ground state can be approximated by a single configuration: one-electron levels shown in Fig. 1 are filled consecutively. The magnetic field dependence of $\mu_{N,1}$ is qualitatively understood by that of the one-electron level occupied by the Nth electron. The behavior of $\mu_{1,1}$ and $\mu_{2,1}$ [$\mu_{3,1}$ and $\mu_{4,1}$] is very similar to that of level $(n, m) = (0, 0)$ [$(0, 1)$] in Fig. 1. The magnetic field dependence of $\mu_{5,1}$ and $\mu_{6,1}$ indicates that the fifth and sixth electrons occupy the level $(0, -1)$ at $\omega_c/\omega_0 < 0.6$ and $(0, 2)$ at $\omega_c/\omega_0 > 0.6$.

Small cusps of $\mu_{4,1}$, $\mu_{5,1}$ ($\mu_{6,1}$, $\mu_{7,1}$) around $\omega_c/\omega_0 = 0.1$ (0.6) are due to the spin-triplet state for $N = 4$ (6) shown in Fig. 2 (b). The exchange interaction makes high spin states in the vicinity of the level crossings (between $(0, 1)$ and $(0, -1)$ at $\omega_c = 0$, $(0, -1)$ and $(0, 2)$ at $\omega_c/\omega_0 = 1/\sqrt{2}$) [10]. This Hund's rule was observed experimentally [1].

With increasing magnetic field, the level spacings become smaller (see Fig. 1) whereas the Coulomb interaction is more effective since the wavefunctions are shrunk. At a critical value of the magnetic field, some electrons start to occupy higher levels to reduce the interaction energy, which results in a transition of the ground state. Such correlation-induced transitions are observed when $\omega_c/\omega_0 > 1.5$.

Figure 3 shows the addition energies ($\mu_{N,1}$ by solid lines, $\mu_{N,i}$ $(i \geq 2)$ by broken lines) until higher magnetic field than in Fig. 2. The transition of the ground state occurs where a broken line crosses a solid line. In the

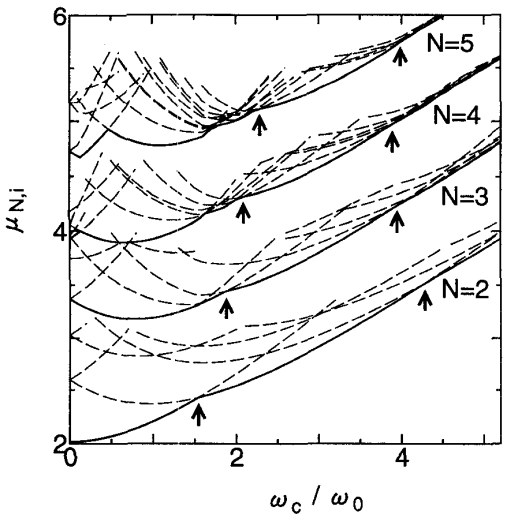

Figure 3: Magnetic field dependence of the addition energies $\mu_{N,i}$ for $N = 2$ to 5. In the abscissa, $\omega_c = eH/m^*c$ is the cyclotron frequency. The unit of $\mu_{N,i}$ is $\hbar\omega_0$. $[e^2/\varepsilon l_0 = \hbar\omega_0.]$

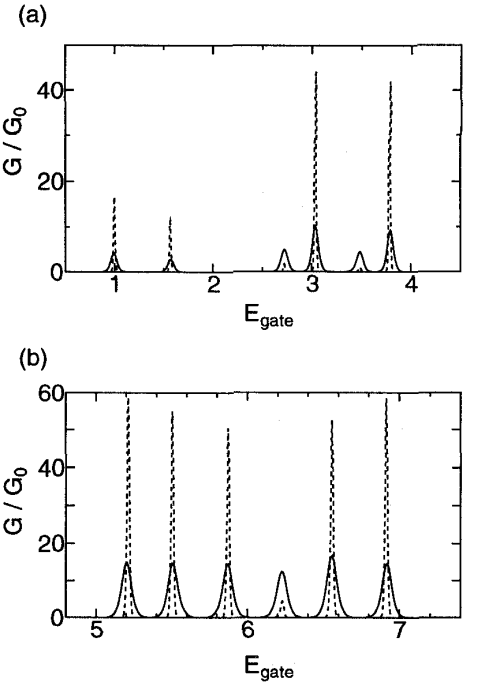

Figure 4: (a) The first to sixth peaks and (b) 7th to 12th peaks of the Coulomb oscillation, in the absence of magnetic field. In the abscissa, $E_{\rm gate} = eV_{\rm gate}$ in units of $\hbar\omega_0$. The temperature is $k_{\rm B}T/\hbar\omega_0 = 0.005$ (dotted lines) and 0.02 (solid lines). In (a), a small anisotropy is taken into account. The transmission amplitude, $T_l^{\rm L/R}$, for the lower level in the second shell (for the first shell) is a quarter (half) of $T_l^{\rm L/R}$ for the upper level in the second shell. In (b), a small anharmonicity is assumed. $T_l^{\rm L/R}$ is independent of the state l in the dot. $[e^2/\varepsilon l_0 = \hbar\omega_0/2.]$

ground state of $N = 2$, for example, two electrons occupy level $(n, m) = (0, 0)$ at low magnetic fields. An electron starts to occupy level $(0, 1)$ at $\omega_c/\omega_0 = 1.54$ [10]. Another transition of the ground state is seen at $\omega_c/\omega_0 = 4.3$. (The total spin changes from $S = 0$ to $S = 1$, and then $S = 0$ [13].) The magnetic field dependence of low-lying excited states as well as the ground state, shown in Fig. 3, is in quantitatively good agreement with experimental results [2].

In a magnetic field range between two arrows in Fig. 3, N electrons are completely spin-polarized ($S = N/2$) and occupy the lowest N levels. This state is called maximum density droplet (MDD). The region becomes narrower with an increase in number of electrons N. This is also in accordance with experimental observation [14]. In the higher side of the region, the MDD state is replaced by a new ground state in which electrons are strongly correlated to each other.

Peak heights of the Coulomb oscillation

The peaks of the Coulomb oscillation usually become lower and broader with an increase in temperature (T). In experimental results [15], however, the heights of third, fifth, 10th and 17th peaks increase with temperature, in the absence of magnetic field. We propose possible mechanisms for the anomalous T dependence of the peak heights [12].

To explain the T dependence of the third and fifth peaks, we make two assumptions. (i) A small anisotropy of the dot splits two degenerate levels in the second shell by $\Delta\varepsilon$ (≈ 1.2 K). (ii) The transmission amplitude, $T_l^{\rm L/R}$ in eq. (7), for the lower level in the second shell is a quarter of that for the upper level. In Fig. 4 (a), we present the first to sixth peaks of the linear-conductance through an artificial atom as a function of gate voltage. The third and fifth peaks are smaller in height at $T = 0.005\hbar\omega_0/k_{\rm B}$ (≈ 0.3 K, dotted lines) than at $T = 0.02\hbar\omega_0/k_{\rm B}$ (≈ 1 K, solid lines).

The reason is as follows. When $k_{\rm B}T \ll \Delta\varepsilon$, the third electron is almost always transported through the lower level in the second shell, which has a smaller transmission probability to the leads than the upper level. With increasing temperature, the upper level contributes more to the third peak, and consequently, the third peak becomes larger. The situation is the same for the fifth peak.

A possible mechanism for the T dependence of the 10th peak (also 17th peak) is "spin blockade" [7]. Figure 4 (b) shows the 7th to 12th peaks of the linear-conductance, in the presence of a small anharmonicity of the confine-

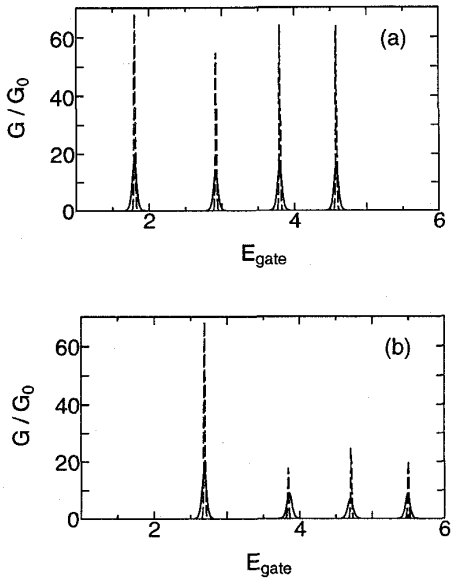

Figure 5: The first to fourth peaks of the Coulomb oscillation, under magnetic fields of (a) $\omega_c/\omega_0 = 3$ and (b) 5. In the abscissa, $E_{\rm gate} = eV_{\rm gate}$ in units of $\hbar\omega_0$. The temperature is $k_BT/\hbar\omega_0 = 0.005$ (broken lines) and 0.02 (solid lines). $[e^2/\varepsilon l_0 = \hbar\omega_0.]$

ment potential [12]. The 10th peak shows the anomalous T dependence for the following reason. The ground state of $N = 9$ has the total spin of $S = 3/2$ whereas that of $N = 10$ has $S = 0$. The 10th peak is very small at low temperatures (dotted line) since the addition of the 10th electron on the dot is forbidden by the spin selection rule. With increasing temperature, electrons are transported more smoothly through transition-allowed excited states, and as a result, the height of the peak grows (solid line).

Correlation effect on transport properties

The electronic correlation can influence the transport properties [8]. Under higher magnetic fields, the correlation effect becomes stronger, which may be reflected in the conductance peaks. Figure 5 shows the first four peaks of the linear-conductance, under magnetic fields of (a) $\omega_c/\omega_0 = 3$ and (b) 5. At $\omega_c/\omega_0 = 3$, where the ground state is MDD for $N = 2$ to 4, all the peaks are nearly the same in height. At $\omega_c/\omega_0 = 5$, electrons are strongly correlated to each other in the ground states. Then the second to fourth peaks are considerably suppressed at low temperatures. In this case, for the addition of the Nth electron on a quantum dot, $N-1$ electrons in the dot have to be redistributed to make the ground state for N electrons. This decreases the transition probability between $\Psi_{N-1,1}$ and $\Psi_{N,1}$ with an electron tunneling $(\Gamma^{\rm L/R}_{N,1;N-1,1})$.

4. Conclusions

The many-body states in an artificial atom and its transport properties have been examined by the numerical studies. The magnetic field dependence of both the ground state and low-lying excited states, obtained by the exact diagonalization method, is in good agreement with experimental results. We have proposed two possible mechanisms for the anomalous T dependence of conductance peak heights. With increasing magnetic field, the correlation effect becomes stronger, which suppresses the conductance considerably.

References

1. S. Tarucha, D. G. Austing, T. Honda, R. J. van der Hage and L. P. Kouwenhoven, Phys. Rev. Lett. **77**, 3613 (1996).
2. L. P. Kouwenhoven, T. H. Oosterkamp, M. W. S. Danoesastro, M. Eto, D. G. Austing, T. Honda and S. Tarucha, Science **278**, 1788 (1997).
3. P. A. Maksym and T. Chakraborty, Phys. Rev. Lett. **65**, 108 (1990).
4. P. A. Maksym and T. Chakraborty, Phys. Rev. B **45**, R1947 (1992).
5. P. Hawrylak, Phys. Rev. Lett. **71**, 3347 (1993).
6. W. Häusler and B. Kramer, Phys. Rev. B **47**, 16353 (1993).
7. D. Weinmann, W. Häusler and B. Kramer, Phys. Rev. Lett. **74**, 984 (1995).
8. K. Jauregui, W. Häusler, D. Weinmann and B. Kramer, Phys. Rev. B **53**, R1713 (1996).
9. Y. Tanaka and H. Akera, Phys. Rev. B **53**, 3901 (1996).
10. M. Eto, Jpn. J. Appl. Phys. **36**, 3924 (1997).
11. Two calculations are performed to determine a many-body state, using different configuration spaces. They are constructed by all the configurations in which N electrons occupy the 15 levels of (n, m) for (i) $2n + |m| \leq 4$, and (ii) $n = 0$ and $-2 \leq m \leq 7$, or $n = 1$ and $0 \leq m \leq 4$, respectively. The solution with the lower energy is adopted.
12. M. Eto, J. Phys. Soc. Jpn. **66**, 2244 (1997).
13. M. Wagner, U. Merkt and A. V. Chaplik, Phys. Rev. B **45**, 1951 (1992).
14. T. H. Oosterkamp, J. W. Janssen, L. P. Kouwenhoven, S. Tarucha, D. G. Austing and T. Honda, private communications.
15. R. J. van der Hage, Ph. D thesis, Delft Univ. of Technology (1996).